

Cite this: *Mater. Adv.*, 2022,  
3, 4531Received 24th March 2022,  
Accepted 2nd May 2022

DOI: 10.1039/d2ma00339b

rsc.li/materials-advances

**We constructed a novel supramolecular gelator (G3) by using acylhydrazone, which exhibited excellent selectivity and ultrasensitive sensing properties toward Mg<sup>2+</sup> in ethanol as well as showed excellent gelation abilities in glycol–H<sub>2</sub>O. Meanwhile, an efficient artificial light-harvesting system (ALHS) has been successfully constructed between G3@Mg-sol or G3@Mg-gel and a hydrophobic fluorescent dye (RhB).**

The development of fluorescent chemosensors for selective recognition of different metal ions has drawn wide attention with their instant response and simple operation, high sensitivity and selectivity.<sup>1</sup> Tremendous amounts of effort have been made toward the development of new fluorescent sensors for metal ions over the past few decades. At present, fluorescent probes have been researched extensively in the fields of analytical and bioimaging, as well as environmental sciences.<sup>2</sup> As an important cation in the human body, Mg<sup>2+</sup> participates in a variety of physiological activities and plays a prominent role in many biological processes.<sup>3</sup> Therefore, selective detection of Mg<sup>2+</sup> ions is of particular significance to the design and synthesis of sensitive and selective sensors. However, designing reliable and sensitive analytical methods for Mg<sup>2+</sup> is still a challenging subject in supramolecular chemistry.

Supramolecular gels are an interesting sort of soft material that display moderate flexibility, which readily allows them to change their shape and properties according to the external conditions, like heat, solvents, pH, light, cations/anions and oxidative/reductive reactions.<sup>4</sup> The key to gel formation is the self-assembly of the low molecular weight gels (LMWGs), interconnected *via* a variety non-covalent interactions, such as hydrogen bonding, van der Waals interactions,  $\pi$ – $\pi$  forces,

## Efficient artificial light-harvesting systems with gel properties formed by ion recognition†

Xinxian Ma,<sup>†</sup> Bo Qiao,<sup>‡</sup> Jinlong Yue, Yutao Geng, Yingshan Lai, Jiali Zhang, Enke Feng, Zhenliang Li and Xingning Han

metal coordination and hydrophobic effects.<sup>5</sup> These excellent properties offered supramolecular gels extraordinary ability to act as smart materials, which has kept on attracting substantial research interest for promising application prospects in tissue engineering, microfluidic devices, chemosensors, drug delivery, optoelectric devices, smart films and biomaterials *etc.*<sup>6</sup>

Inspired by photosynthesis in nature, artificial light-harvesting systems (LHSs) can be constructed, which rely on the Förster resonance energy transfer (FRET) processes from donor to acceptor for harvesting, funneling and utilizing light energy.<sup>7</sup> In order to achieve an artificial supramolecular LHS, two key factors are considered for an efficient FRET system: (1) the emission spectra of the donor fluorophore must overlap well with the absorption spectrum of the acceptor fluorophore; and (2) the donor and acceptor should be close to each other (within 10 nm).<sup>8</sup> Li and Yang *et al.* constructed artificial light harvesting systems based on lower-rim dodecylmodified sulfonatocalix arene (SC<sub>4</sub>AD) and a naphthyl-1,8-diphenyl pyridinium derivative (NPS) with AIEE as a donor and Nile blue (NiB) as an acceptor. Meanwhile, the NPS–SC<sub>4</sub>AD–NiB system exhibits an ultrahigh antenna effect (33.1) at a donor/acceptor ratio of 250:1.<sup>9</sup> Yang and co-workers reported a dual-donor (TPE-containing metallacycle 3 and DSA-containing dinitrile guest 4) supramolecular artificial LHS through host–guest interactions, metal–ligand coordination interactions and hydrophobic interactions. Remarkably, the dual-donor artificial LHS exhibited higher energy transfer efficiency and antenna effects.<sup>10</sup>

In this work, we proposed and reported a structurally simple and novel gelator (G3, Scheme 1) based on our previous literature.<sup>11</sup> The gelator G3 could self-assemble to form a supramolecular gel G3–gel in glycol and water solvents that showed excellent selectivity and sensitivity for identifying Mg<sup>2+</sup>. Based on the above characteristics, we designed two novel efficient artificial light-harvesting supramolecular assembly systems with G3@Mg-sol and RhB, G3@Mg-gel and RhB.

The response properties of G3 in ethyl alcohol were researched by adding positive ions: K<sup>+</sup>, Na<sup>+</sup>, Mn<sup>2+</sup>, Ni<sup>2+</sup>, Pb<sup>2+</sup>,

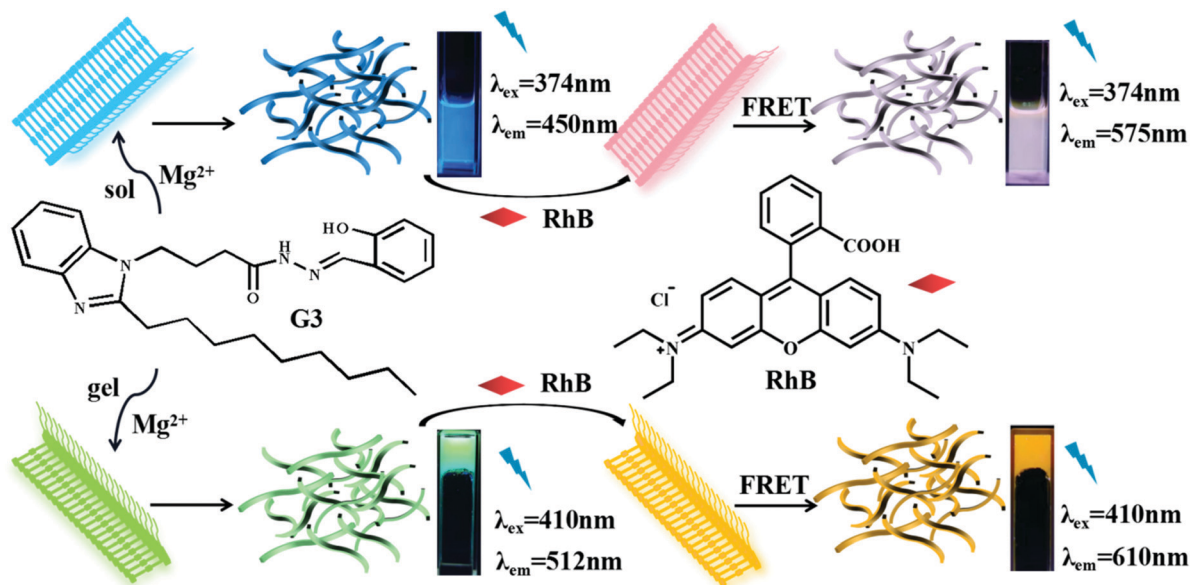
College of Chemistry and Chemical Engineering, Ningxia Normal University,  
Guyuan 756000, People's Republic of China. E-mail: maxinxian@163.com;

Tel: +86-954 2079637

† Electronic supplementary information (ESI) available. See DOI: <https://doi.org/10.1039/d2ma00339b>

‡ These authors contributed equally to this work. They should thus be considered co-first authors.





Scheme 1 Construction of the G3@Mg-sol/RhB and G3@Mg-gel/RhB light-harvesting system.

$\text{Cd}^{2+}$ ,  $\text{Co}^{2+}$ ,  $\text{Zn}^{2+}$ ,  $\text{Hg}^{2+}$ ,  $\text{Cr}^{3+}$ ,  $\text{Mg}^{2+}$ ,  $\text{Cu}^{2+}$ ,  $\text{Fe}^{3+}$ ,  $\text{Al}^{3+}$  and  $\text{Ag}^{+}$  by fluorescence spectra. Only  $\text{Mg}^{2+}$  could induce the fluorescence intensity of G3 to turn on obviously. As depicted in Fig. 1a, gelator G3 showed a faint blue fluorescence emission at 450 nm in the ethanol medium. However, the addition of  $\text{Mg}^{2+}$

displayed a bright blue fluorescence and led to a distinct increase in the corresponding emission intensity, but the concentration increases of other positive ions couldn't trigger any significant changes in the fluorescence spectrum when excited at 374 nm. Interestingly,  $\text{Al}^{3+}$  causes fluorescence enhancement on the emission intensity compared with the primitive emission spectrum. But, the emission peak at 450 nm was significantly weakened as time goes by, as illustrated in Fig. 1c. Simultaneously, the emission peak was slightly enhanced when  $\text{Mg}^{2+}$  was added under the same conditions above, as illustrated in Fig. 1d. Therefore, G3 exhibited specific selectivity for  $\text{Mg}^{2+}$ . The detection limit of the G3 for  $\text{Mg}^{2+}$  is  $1.0 \times 10^{-6} \text{ mol L}^{-1}$ , which was obtained by fluorescence titrations and demonstrated high detection sensitivity for  $\text{Mg}^{2+}$ . In order to understand the binding stoichiometry between G3 and  $\text{Mg}^{2+}$ , the Job's plot (Fig. 1b) was revealed based on a continuous variation method. The maximum emission value appears at the mole fraction of 0.5, which exhibited that G3 and  $\text{Mg}^{2+}$  formed a 1 : 1 ligand–metal complex. According to the IR spectra (Fig. S4, ESI<sup>†</sup>), the binding mode between the G3 and  $\text{Mg}^{2+}$  was investigated. In the IR spectrum of G3, the peaks at  $3182 \text{ cm}^{-1}$  and  $3066 \text{ cm}^{-1}$  were ascribed to the phenol –OH and –NH stretching, respectively. It was found that the peak would move after  $\text{Mg}^{2+}$  binding, indicating that the phenol O and imino N atoms complexed with  $\text{Mg}^{2+}$ . And, we hypothesized the possible luminescence mechanism of the G3@Mg-gel in Fig. S5 (ESI<sup>†</sup>). In order to study the self-assembly driving forces of G3 and G3@Mg-sol, X-ray diffraction analysis was carried out. The XRD patterns of G3@Mg-gel (Fig. S6, ESI<sup>†</sup>) showed a characteristic peak at  $2\theta = 28.806$  with  $d$ -spacings of 0.31 nm, supporting the presence of  $\pi$ – $\pi$  stacking. The gelator G3 and G3@Mg-gel showed  $d$ -spacings of 1.639 nm and 1.82 nm at  $2\theta = 5.384^\circ$  and  $5.41^\circ$  in addition to remarkable

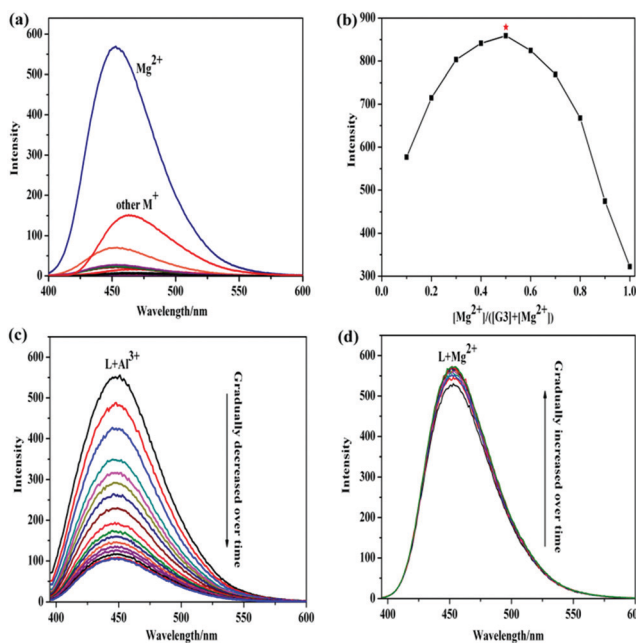


Fig. 1 (a) Fluorescence spectra of G3 ( $1 \times 10^{-3} \text{ mol L}^{-1}$ ) in ethanol with different metal cations ( $\text{Zn}^{2+}$ ,  $\text{Al}^{3+}$ ,  $\text{Cu}^{2+}$ ,  $\text{Cd}^{2+}$ ,  $\text{Co}^{2+}$ ,  $\text{Fe}^{3+}$ ,  $\text{Cr}^{3+}$ ,  $\text{Fe}^{2+}$ ,  $\text{Hg}^{2+}$ ,  $\text{Mg}^{2+}$ ,  $\text{Mn}^{2+}$ ,  $\text{Na}^{+}$ ,  $\text{Ni}^{2+}$ , and  $\text{Pb}^{2+}$ , excited at 374 nm); (b) a Job's plot indicating the 1 : 1 stoichiometry of G3@Mg-sol (the total concentration of G3 and  $\text{Mg}^{2+}$  is  $1 \times 10^{-4} \text{ mol L}^{-1}$ ); (c) time-dependent fluorescence spectra of the G3@Al-sol complex; (d) time-dependent fluorescence spectra of the G3@Mg-sol complex.



$\pi$ - $\pi$  interactions. These results show that the self-assembly mode of G3@Mg-gel is different from that of G3, and this is due to the coordination effect of G3 with  $Mg^{2+}$ .

Considering an efficient FRET system, we initially measured the emission spectrum of G3@Mg-sol and the absorption of RhB to construct a supramolecular light-harvesting system. As demonstrated in Fig. 2a, the fluorescence emission of the G3@Mg-sol complex overlaps well with the absorption band of RhB, ensuring that efficient FRET occurs. Hence, an efficient light-harvesting system (G3@Mg-sol/RhB) is expected to occur when RhB could be loaded into the G3@Mg-sol assembly. Actually, as shown in Fig. 2b, with the increase of the ratio [G3@Mg-sol]/[RhB] from 1000:1 to 100:1, the fluorescence emission of G3@Mg-sol at 450 nm decreased gradually, and the emission intensity of the RhB at 575 nm increased obviously when excited at 374 nm. Simultaneously, a remarkable color change was observed from blue to pink by the naked eye (Fig. 2b, inset). The fluorescence decay of G3@Mg-sol was fitted by a double-exponential decay with the fluorescence lifetime of  $\tau_1 = 0.51$  ns and  $\tau_2 = 2.43$  ns (Fig. S7 and S8a, ESI<sup>†</sup>). In the G3@Mg-sol/RhB assembly, the fluorescence lifetimes changed into  $\tau_1 = 2.31$  ns followed a double exponential decay (Fig. S7 and S8b, ESI<sup>†</sup>). Furthermore, the fluorescence quantum yield of G3@Mg-sol/RhB was 15.46% (Fig. S9, ESI<sup>†</sup>), probably due to efficient energy transfer to RhB rather than direct emission of G3@Mg-sol. In addition, the energy transfer efficiency ( $\Phi_{ET}$ ) and antenna effect (AE) are primary empirical parameters for evaluating the performance of such artificial light-harvesting systems. In particular, the  $\Phi_{ET}$  and AE of G3@Mg-sol/RhB were calculated as 44.9% (Fig. S11, ESI<sup>†</sup>) and 5.3 (Fig. S12, ESI<sup>†</sup>) at the donor/acceptor molar ratio = 50:1. Such results demonstrate that the G3@Mg-sol/RhB is an efficient light harvesting system.

Initially, we researched whether the gelator is able to assemble gels in various solvents (Table S1, ESI<sup>†</sup>). The compound G3 was added to diverse solvents, the mixed solution was heated until it dissolved, then was left standing and cooled to room temperature, forming a stable gel. The gel characteristics of compound G3 were examined according to the inverted

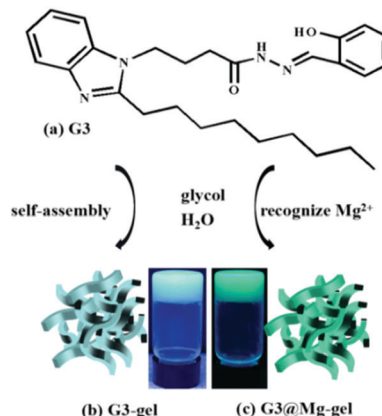


Fig. 3 (a) Gelator G3, (b) G3-gel, and (c) G3@Mg-gel. Inset: Photographs of the G3-gel and G3@Mg-gel upon irradiation using 365 nm UV light.

tube method. Among these solvents, it's worth noting that gelator G3 could self-assemble into a stable supramolecular gel G3-gel in ethylene glycol and aqueous solution (volume ratio = 7:3) with the lowest critical gelation concentration (CGC) of 2.5% ( $10 \text{ mg mL}^{-1} = 1\%$ ) and the highest gel-sol transition temperature ( $T_{gel}$ ) of about  $85^\circ\text{C}$ . However, it takes about six hours to complete it, which is a long process. Besides, the G3-gel was thermally reversible (Fig. S13a and b, ESI<sup>†</sup>). Interestingly, G3 showed excellent gelation abilities in glycol and  $H_2O$  when  $Mg^{2+}$  was added. Compared with the G3-gel, the G3@Mg-gel exhibited a distinct fluorescence color change from pale blue (Fig. 3b) to bright green (Fig. 3c) when irradiated with UV light at 365 nm. The morphological structure of the G3-gel was further investigated by SEM (scanning electron microscopy), and a loose fibrous sheet nature was observed, as shown in Fig. S13c and d (ESI<sup>†</sup>).

Compared with the solution state (G3@Mg-sol), the maximum absorption of G3@Mg-gel manifested a bathochromic-shift (Fig. S14, ESI<sup>†</sup>), indicating that a J-type  $\pi$ - $\pi$  aggregation effect exists in self-assembly. Considering the eminent luminescence performance of G3@Mg-gel, RhB as an acceptor could be loaded into the supramolecular gel to achieve efficient energy transfer, because the absorption of G3@Mg-gel overlaps with the emission of RhB (Fig. S15a, ESI<sup>†</sup>), which makes a supramolecular gel light harvesting system from G3@Mg-gel to RhB (G3@Mg-gel/RhB). As shown in Fig. S15b (ESI<sup>†</sup>), the fluorescence intensity at 512 nm decreased and a new emission peak at 610 nm appeared simultaneously with 410 nm excitation, when the acceptor RhB was added into G3@Mg-gel. The Stokes shift reached 35 nm and a remarkable color change was observed from pink to orange by the naked eye, compared with the light-harvesting system G3@Mg-sol/RhB. The decay curve of G3@Mg-gel followed a double exponential decay with a fluorescence lifetime of  $\tau_1 = 1.18$  ns and  $\tau_2 = 6.83$  ns (Fig. S16 and S17a, ESI<sup>†</sup>). In the G3@Mg-gel/RhB system, the fluorescence lifetimes decreased to  $\tau_1 = 1.14$  ns and  $\tau_2 = 6.05$  ns (Fig. S16 and S17b, ESI<sup>†</sup>). Furthermore, the fluorescence quantum yield of G3@Mg-gel/RhB was 30.66% (Fig. S17, ESI<sup>†</sup>), and the  $\Phi_{ET}$  of

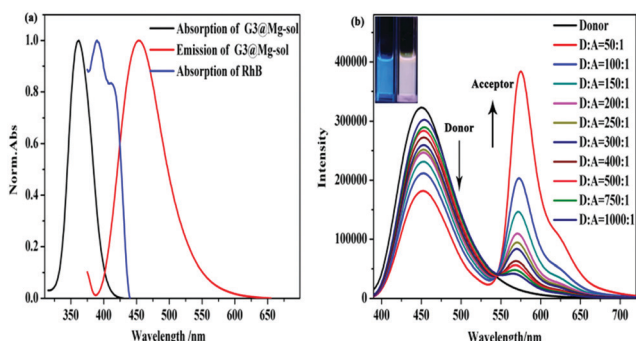


Fig. 2 (a) Normalized absorption and emission spectrum of G3@Mg-sol, and absorption spectrum of RhB. (b) Fluorescence spectrum of G3@Mg-sol/RhB ([G3@Mg-sol] =  $1 \mu\text{M}$ , [RhB] =  $0.02 \mu\text{M}$ ) in ethanol and water with different concentrations of RhB (Inset: photographs of G3@Mg-sol and G3@Mg-sol/RhB).



G3@Mg-gel/RhB was calculated as 99.99% at the donor/acceptor molar ratio = 50:1.

In summary, we have explored and developed an efficient artificial light harvesting system with gel properties formed by ion recognition. We developed a fluorescent probe which displayed a distinct response to  $Mg^{2+}$ . The G3@Mg-sol/RhB artificial light-harvesting system was successfully constructed and presented the highest fluorescence quantum yield and energy transfer efficiency at the donor/acceptor molar ratio = 50:1. Besides, G3@Mg-gel showed green fluorescence in glycol-H<sub>2</sub>O under 365 nm UV light. At this optimal ratio, the artificial light harvesting system (G3@Mg-gel/RhB) exhibits better fluorescence quantum yield (30.66%) and higher energy transfer efficiency (99.99%) with G3@Mg-gel as the donor. This work associates ion recognition of the gel with light-harvesting systems.

## Conflicts of interest

There are no conflicts to declare.

## Acknowledgements

This work was supported by the National Natural Science Foundation of China (No. 21961029), The Natural Science Foundation of Ningxia, China (No. 2020AAC02031), Key Research Foundation of Department of Science and Technology of Ningxia, China (No. 2021BEE03019), The Science and Technology Foundation of Guyuan, China (No. 2021GYKYF003), and Research Award Fund for First-class Discipline Construction (Education Discipline) in Higher Education Institutions of Ningxia, China (No. NXYLXK2021B10), which are gratefully acknowledged.

## Notes and references

- (a) P. Roy, Fluorescent chemosensors based on 4-methyl-2,6-diformylphenol, *Coord. Chem. Rev.*, 2020, **427**, 213562; (b) H. So, H. Lee, G. D. Lee, M. Kim, M. H. Lim, K. T. Kim and C. Kim, A thiourea-based fluorescent chemosensor for bioimaging Hypochlorite, *J. Ind. Eng. Chem.*, 2020, **89**, 436–441; (c) S. Wang, B. T. Zhu, B. Y. Wang, P. W. Fan, Y. X. Jiu, M. Zhang, L. R. Jiang and J. T. Hou, A highly selective phenothiazine-based fluorescent chemosensor for phosgene, *Dyes Pigm.*, 2020, **173**, 107933; (d) P. S. Zhang, J. Chen, F. H. Huang, Z. Q. Zeng, J. Hu, P. G. Yi, F. Zeng and S. Z. Wu, One-pot fabrication of polymernanoparticle-based chemosensors for  $Cu^{2+}$  detection in aqueous media, *Polym. Chem.*, 2013, **4**, 2325–2332.
- (a) T. S. Wang, N. Zhang, W. Bai and Y. Y. Bao, Fluorescent chemosensors based on conjugated polymers with N-heterocyclic moieties: two decades of progress, *Polym. Chem.*, 2020, **11**, 3095–3114; (b) Z. Y. Zhu, J. B. Huang and Y. Yan, A human vision inspired adaptive platform for one-on-multiple recognition, *Chem. Commun.*, 2019, **55**, 4829–4832.
- (a) J. C. Qin, M. Wang, Z. H. Fu and Z. H. Zhang, Design and synthesis of a solvent-dependent fluorescent probe for dual selective detection of  $Mg^{2+}$  ion and  $Zn^{2+}$  ion, *J. Photochem. Photobiol., A*, 2021, **405**, 112965; (b) Y. C. Huang, F. Jin, Y. Funato, Z. J. Xu, W. L. Zhu, J. Wang, M. X. Sun, Y. M. Zhao, Y. Yu, H. Miki and M. Hattori, Structural basis for the  $Mg^{2+}$  recognition and regulation of the CorC  $Mg^{2+}$  transporter, *Sci. Adv.*, 2021, **7**(7), DOI: [10.1126/sciadv.abe6140](https://doi.org/10.1126/sciadv.abe6140); (c) A. Tomita, M. Zhang, F. Jin, W. H. Zhuang, H. Takeda, T. Maruyama, M. Osawa, K. Hashimoto, H. Kawasaki, K. Ito, N. Dohmae, R. Ishitani, I. Shimada, Z. Yan, M. Hattori and O. Nureki, ATP-dependent modulation of MgtE in  $Mg^{2+}$  Homeostasis, *Nat. Commun.*, 2017, **8**, 1–11.
- (a) F. Xie, L. Qin and M. H. Liu, A dual thermal and photo-switchable shrinking-swelling supramolecular peptide dendron gel, *Chem. Commun.*, 2016, **52**, 930–933; (b) L. Qin, P. F. Duan, F. Xie, L. Zhang and M. H. Liu, A metal ion triggered shrinkable supramolecular hydrogel and controlled release by an amphiphilic peptide dendron, *Chem. Commun.*, 2013, **49**, 10823–10825; (c) J. W. Steed, Anion-tuned supramolecular gels: a natural evolution from urea supramolecular chemistry, *Chem. Soc. Rev.*, 2010, **39**, 3686–3699; (d) D. Liu, S. H. Zang, R. R. Xue, J. H. Yang, L. Z. Wang, J. B. Huang and Y. Yan, Coordination-Triggered Hierarchical Folate/Zinc Supramolecular Hydrogels Leading to Printable Biomaterials, *ACS Appl. Mater. Interfaces*, 2018, **10**, 4530–4539; (e) X. F. Ji, R. T. Wu, L. L. Long, X. S. Ke, C. X. Guo, Y. J. Ghang, V. M. Lynch, F. H. Huang and J. L. Sessler, Encoding, Reading, and Transforming Information Using Multifluorescent Supramolecular Polymeric Hydrogels, *Adv. Mater.*, 2018, **30**, 1705480; (f) F. H. Huang, X. Zhang and B. Z. Tang, Stimuli-responsive materials: a web themed collection, *Mater. Chem. Front.*, 2019, **3**, 10–11; (g) L. Yang, X. W. Sun, Y. M. Zhang, Z. H. Wang, W. Zhu, Y. Q. Fan, T. B. Wei, H. Yao and Q. Lin, A bi-component supramolecular gel for selective fluorescence detection and removal of  $Hg^{2+}$  in water, *Soft Matter*, 2019, **15**, 9547–9552; (h) H. Yao, X. T. Kan, Q. Zhou, Y. B. Niu, Y. M. Zhang, T. B. Wei and Q. Lin, Lanthanide-Mediated Cyclodextrin-Based Supramolecular Assembly-Induced Emission Xerogel Films: A Transparent Multicolor Photoluminescent Material, *ACS Sustainable Chem. Eng.*, 2020, **8**, 13048–13055.
- (a) Y. T. Sang and M. H. Liu, Nanoarchitectonics through supramolecular gelation: formation and switching of diverse nanostructures, *Mol. Syst. Des. Eng.*, 2019, **4**, 11–28; (b) J. Zhou, G. C. Yu and F. H. Huang, Porous organic polymers for Li-chemistry-based batteries: functionalities and characterization studies, *Chem. Soc. Rev.*, 2017, **46**, 7021–7053; (c) K. Q. Liu, S. Gao, Z. Zheng, X. L. Deng, S. Mukherjee, S. S. Wang, H. Xu, J. Q. Wang, J. F. Liu, T. Y. Zhai and Y. Fang, Spatially Confined Growth of Fullerene to Super-Long Crystalline Fibers in Supramolecular Gels for High-Performance Photodetector, *Adv. Mater.*, 2019, **31**, 1808254.
- (a) M. H. Liu, G. H. Ouyang, D. Niu and Y. T. Sang, Supramolecular gelatons: towards the design of molecular gels, *Org. Chem. Front.*, 2018, **5**, 2885–2900; (b) X. F. Ji, B. B. Shi,



- H. Wang, D. Y. Xia, K. C. Jie, Z. L. Wu and F. H. Huang, Double layer 3D codes: fluorescent supramolecular polymeric gels allowing direct recognition of the chloride anion using a smart phone, *Adv. Mater.*, 2015, **27**, 8062–8066.
- 7 (a) T. X. Xiao, L. L. Zhang, H. R. Wu, H. W. Qian, D. X. Ren, Z. Y. Li and X. Q. Sun, Supramolecular polymer-directed light-harvesting system based on a stepwise energy transfer cascade, *Chem. Commun.*, 2021, **57**, 5782–5785; (b) D. Q. Zhang, W. Yu, S. W. Li, Y. Xia, X. Y. Li, Y. R. Li and T. Yi, Artificial Light-Harvesting Metallacycle System with Sequential Energy Transfer for Photochemical Catalysis, *J. Am. Chem. Soc.*, 2021, **143**, 1313–1317; (c) T. X. Xiao, W. W. Zhong, L. Zhou, L. X. Xu, X. Q. Sun, R. B.-P. Elmesb, X. Y. Hu and L. Y. Wang, Artificial light-harvesting systems fabricated by supramolecular host-guest interactions, *Chin. Chem. Lett.*, 2019, **30**, 31–36.
- 8 (a) T. X. Xiao, H. R. Wu, G. P. Sun, K. Diao, X. Y. Wei, Z. Y. Li, X. Q. Sun and L. Y. Wang, An efficient artificial light-harvesting system with tunable emission in water constructed from a H-bonded AIE supramolecular polymer and Nile Red, *Chem. Commun.*, 2020, **56**, 12021–12024; (b) X. M. Chen, Q. Cao, H. K. Bisoyi, M. Wang, H. Yang and Q. Li, An Efficient Near-Infrared Emissive Artificial Supramolecular Light-Harvesting System for Imaging in the Golgi Apparatus, *Angew. Chem., Int. Ed.*, 2020, **59**, 10493–10497; (c) M. Hao, G. P. Sun, M. Z. Zuo, Z. Q. Xu, Y. Chen, X. Y. Hu and L. Y. Wang, A Supramolecular Artificial Light-Harvesting System with Two-Step Sequential Energy Transfer for Photochemical Catalysis, *Angew. Chem., Int. Ed.*, 2019, **59**, 10095–10100; (d) T. X. Xiao, C. Bao, L. L. Zhang, K. Diao, D. X. Ren, C. X. Wei, Z. Y. Li and X. Q. Sun, An artificial light-harvesting system based on the ESIPT–AIE–FRET triple fluorescence mechanism, *J. Mater. Chem. A*, 2022, **10**, 8528.
- 9 J. J. Li, H. Y. Zhang, X. Y. Dai, Z. X. Liu and Y. Liu, A highly efficient light-harvesting system with sequential energy transfer based on a multicharged supramolecular assembly, *Chem. Commun.*, 2020, **56**, 5949–5952.
- 10 Y. X. Hu, P. P. Jia, C. W. Zhang, X. D. Xu, Y. F. Niu, X. L. Zhao, Q. Xu, L. Xu and H. B. Yang, A supramolecular dual-donor artificial light-harvesting system with efficient visible light-harvesting capacity, *Org. Chem. Front.*, 2021, **8**, 5250–5257.
- 11 (a) X. X. Ma, D. W. Yu, N. Tang and J. C. Wu, Tb<sup>3+</sup>-containing supramolecular hydrogels: luminescence properties and reversible sol-gel transitions induced by external stimuli, *Dalton Trans.*, 2014, **43**, 9856–9859; (b) X. X. Ma, B. Qiao, Y. S. Lai, Y. T. Geng, J. L. Le, E. K. Feng, X. N. Han and M. H. Liu, Intelligent writable material based on a supramolecular self-assembly gel, *Soft Matter*, 2021, **17**, 1463–1467.

